INTERNATIONAL JOURNAL OF OPTIMIZATION IN CIVIL ENGINEERING
Int. J. Optim. Civil Eng., 2018; 8(2):275-293

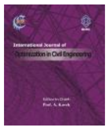

APPLICATION OF FINITE ELEMENT MODEL UPDATING FOR DAMAGE ASSESSMENT OF SPACE STRUCTURE USING CHARGED SYSTEM SEARCH ALGORITHM

H. Safari and A. Gholizad*, †
Department of Civil Engineering, University of Mohaghegh Ardabili, Ardabil, Iran

ABSTRACT

Damage assessment is one of the crucial topics in the operation of structures. Multiplicities of structural elements and joints are the main challenges about damage assessment of space structure. Vibration-based damage evaluation seems to be effective and useful for application in industrial conditions and the low-cost. A method is presented to detect and assess structural damages from changes in mode shapes. First, the mechanism of using two-dimensional continuous wavelet transform is applied for damage localization. Second, finite element model updating technique is utilized as an inverse optimization problem by applying the charged system search algorithm to assess the damage in each element sited in the first stage. The study indicates the potentiality of the developed code to assess the damages of space structures without concerning about the size and shape of structure. A series of numerical examples with different damage scenarios have been carried out in the double layer space structures and the results confirm the reliability and applicability of introduced method.

Keywords: damage detection, 2D continuous wavelet transform, finite element model updating, space structure, charged system search algorithm.

Received: 10 July 2017; Accepted: 7 September 2017

1. INTRODUCTION

Damage detection using structural modal identification methods is based on the premise that damage is manifested as a loss of effective stiffness over one or more regions of the structure. These damages may endanger structure’s integrity and functionality and need to be accurately detected [1].

Vibration based Structural Health Monitoring (SHM) became an interesting research topic in structural mechanics around 30 years ago. Vibration methods are based on the fact

*Corresponding author: University of Mohaghegh Ardabili, Ardabi, Iran
†E-mail address: gholizad@uma.ac.ir (A. Gholizad)

that the reduction of stiffness due to damage affects the dynamic response of structure. Alteration of the vibration characteristics of the structure, such as the natural frequency, displacement, mode shapes and damping ratios are signs to observe the damage in the structure [2].

Vibration based methods are typified by Fourier transform [3,4], wavelet transform [5,6], time-frequency analysis [7,8], and intelligent computation [9]. Wavelet transform background comes from the beginning of the last century [10], and its development as an engineering signal processing analysis tool for SHM is rather new [11]. Wavelet analysis is an efficient methodology which has found wide applications in structural health monitoring (SHM) problems. Wavelet transform is mainly attractive because of its ability to compress and encode information, to reduce noise, or to detect any local singular behavior of a signal.

Wavelet-based methods have been applied by researchers for detection and localization of damages in one-dimensional structural parts (beams) [12-14] and 2D plane problems (plate) [15-18].

An appropriate feature must be sensitive enough to damage, but rather insensitive to environmental and operational effects; hence, selecting a suitable damage indicator feature is a major issue in this approach. The literatures about the vibration based damage identification methods are abundant and several damages sensitive features have been proposed in the previous research [19-21]. Among different structural responses that can be used as measures of structural damage, modal parameters enjoy the benefit of being independent of external excitation [22]. If a modal analysis is performed, then wavelet analysis can be applied to mode shapes or their derivatives to detect changes induced by damage.

Space structures, which enable the designers to cover large spans as sports stadiums, assembly halls, exhibition centers, swimming pools, shopping centers and industrial buildings have been widely applied by structural and architectural engineers in the recent decades. According to the application of structure, various types of space frames like geodesic dome, double layer grid and pyramid could be designed. In the prior methods introduced by other researchers for damage detection of truss like structures, size of structure, differences in geometric patterns and verity of shape were the key problems to limit the application of these methods [1,23-25].

To reduce the computational costs and time, the mechanism of using two dimensional continuous wavelet transform (2D- CWT) is applied by exploiting the concept of simulating the mode shape of space structure to a 2D spatially distributed signal for damage localization of space structure [2].

In the last few decades, techniques based on finite element model updating (FEMU) have been widely developed for vibration-based damage detection. The basic idea is to change the properties of the numerical model to fit the values provided by experimental data, identifying damaged regions and the extent of damage on the structure. In other words, the optimization algorithm seeks the optimal reduction factors of element's stiffness to achieve a predefined performance in terms of the modal parameters defined by the experimental data [26]. SR Shiradhonkar and M. Shrikhande [27] used the frequency-domain decomposition and empirical transfer function estimates to identify the modal parameters. They found that a combination of system identification techniques with sensitivity based finite element model updating can potentially locate and quantify the damage in a moment resistant frame. YZ Fu, et al. [28] used the inverse response sensitivity- based finite element model updating approach with the penalty function method with Tikhonov regularization to identify local damages of the plate in the time domain. A Majumdar, et al. [23] formulate the inverse problem in terms of optimization and utilized a solution technique employing ant colony optimization to detect and assess structural damages from changes in natural frequencies. The developed code is used to assess damages of truss like structures using first few natural frequencies. An improvement in the hybrid Pincus-Nelder-Mead optimization algorithm (P-NMA) which enables to solve the target optimization problem of vibration-based damage detection is proposed by [29], and the results of a beam modeled with 25 finite elements were compared to those obtained by the P-NMA and the meta heuristic harmony search algorithm. ZH Ding, et al. [24] used artificial bee colony algorithm with hybrid search strategy based on an objective function established in the frequency domain for damage detection on a truss and plate structures. SM Seyedpoor [25] proposed a two-stage method of determining the location and extent of multiple structural damages. First, the damage is located using the concept of modal strain energy and second; the particle swarm optimization is utilized to determine the extent of damaged elements. The method is assessed by a planar truss with 31 elements.

This paper presents a framework for SHM and damage assessment of space structure. In the first stage, the mechanism of using 2D- CWT is applied for damage localization of space structure [2]. In the second stage, finite element model updating (FEMU) technique is utilized as an inverse optimization problem by applying the charged system search (CSS) algorithm [30] to assess the amount of damage of each element sited in the first stage. Numerical results show the high efficiency of the proposed method for accurately identifying the extent of multiple structural damages.

2. THEORETICAL BACKGROUND

2.1 Two-dimensional continuous wavelet transform

Wavelet analysis provides a powerful tool to characterize the local features of a signal. Unlike the Fourier transform, where the function used as the basis of decomposition is always a sinusoidal wave, other basis functions can be selected for wavelet shape according to the features of the signal.

The two-dimensional CWT (2D-CWT) is a natural extension of the one-dimensional CWT, with the translation parameter being a vector in the plane. As in the 1D case, a 2D wavelet is an oscillatory, real or complex-valued function $\psi(\vec{x})\epsilon\, L^2(R^2, d^2\vec{x})$ satisfying the admissibility condition on real plane $\vec{x}\,\epsilon\, R^2$, $L^2(R^2, d^2\vec{x})$ denotes the Hilbert space of measurable, square integrable 2D functions on the plane. If ψ is regular enough as in most cases, the admissibility condition can be expressed as:

$$\psi(\vec{0}) = 0 \Leftrightarrow \int_{R^2} \psi(\vec{x}) d^2\vec{x} = 0 \tag{1}$$

Function $\psi(\vec{x})$ is called mother wavelet and usually localized in both the position and frequency domains. The mother wavelet ψ can be transformed in the plane to generate a family of wavelet $\psi_{a,\vec{b},\theta}(\vec{x})$. A transformed wavelet $\psi_{a,\vec{b},\theta}(\vec{x})$ under translation by a vector $\vec{b}$, dilation by a scaling factor a, and rotation by an angel θ can be derived as [31]:

$$\psi_{a,\vec{b},\theta}(\vec{x}) = a^{-1}\psi\left(r_{-\theta}\left(\frac{\vec{x}-\vec{b}}{a}\right)\right) \quad a > 0, \vec{b}, \theta \epsilon R^2 \tag{2}$$

Given a 2D signal $f(\vec{x})\epsilon L^2(R^2, d^2\vec{x})$, its 2D-CWT (with respect to the wavelet ψ) $Wf(a,\vec{b},\theta)$ is the scalar product of $f(\vec{x})$ with the transformed wavelet $\psi_{a,\vec{b},\theta}$ and considered as a function of $(a,\vec{b},\theta)$ as:

$$\mathrm{Wf}(a,\vec{b},\theta) = \langle f, \psi_{a,\vec{b},\theta}\rangle = \frac{1}{\sqrt{a}}\int_{-\infty}^{+\infty} f(\vec{x})\psi^*\left(r_{-\theta}\left(\frac{\vec{x}-\vec{b}}{a}\right)\right)d^2\vec{x} \tag{3}$$

where the ψ^* denotes the complex conjugate and $r_{-\theta}$ is the 2D rotation matrix as:

$$r_{-\theta} = \begin{bmatrix} \cos(\theta) & -\sin(\theta) \\ \sin(\theta) & \cos(\theta) \end{bmatrix} \tag{4}$$

The 2D-CWT is a space scale representation of a plane and acts as a local filter with scale and position. If the wavelet is isotropic, there is no dependence on angle in the analysis. The Mexican hat wavelet is an example of an isotropic wavelet. Isotropic wavelets are suitable for point wise analysis of a 2D system. If the wavelet is anisotropic, there is a dependence on angle in the analysis, and the 2D-CWT acts a local filter with scale, position, and angle. The morlet wavelet is an example of an anisotropic wavelet. In the Fourier domain, this means that the spatial frequency support of the wavelet is a convex cone with the apex at the origin. Anisotropic wavelets are suitable for detecting directional feature.

The point wise nature of the 2D damage detection in the space structure is made the isotropic wavelets suitable for this kind of structure. The chosen wavelet function is isotropic Mexican hat wavelet, and the scaled is equal to 2. Wavelet computation is performed using MATLAB code.

The denoising and filtering capability of the isotropic 2D-CWT provides us with an important analysis tool in practice. The Mexican hat wavelet is real and isotropic. The 1D Mexican hat wavelet is the second derivative of the Gaussian function. Likewise, the 2D Mexican hat wavelet is the Laplacian of the 2D Gaussian function. It was first proposed by EC Hildreth [32] as a differential-smooth operator for their edge contours detection theory. Its expression in the position domain is given as follows [15]:

$$\psi(\vec{x}) = (2 - |\vec{x}|^2)\exp\left(-\frac{1}{2}|\vec{x}|^2\right) \tag{5}$$

2.2 Charged system search algorithm

The Charged System Search (CSS) algorithm is based on the Coulomb and Gauss laws from electrical physics and the governing laws of motion from the Newtonian mechanics. This algorithm can be considered as a multi-agent approach, where each agent is a Charged Particle (CP). In this section, CSS is represented briefly. The CSS algorithm can be summarized as follows:

Level 1. Initialization

Step 1. Initialization. The initial positions of CPs are determined randomly in the search space as:

$$x_{i,j}^{(0)} = x_{i,min} + rand.\left(x_{i,max} - x_{i,min}\right), i = 1, 2, \ldots, n \tag{6}$$

where $x_{i,j}^{(0)}$ determines the initial value of the *i*th variable for the *j*th CP; $x_{i,min}$ and $x_{i,max}$ are the minimum and the maximum allowable values for the *i*th variable; *rand* is a random number in the interval [0,1]; and *n* is the number of variables. The initial velocities of charged particles are set to zero

$$v_{i,j}^{(0)} = 0, \quad i = 1, 2, \ldots, n \tag{7}$$

The magnitude of the charge is defined considering the quality of its solution, as follows:

$$\mathrm{q_i} = \frac{\mathrm{fit(i) - fitworst}}{\mathrm{fitbest - fitworst}} \quad \mathrm{i} = 1,2,3 \ldots\ldots, \mathrm{N} \tag{8}$$

where *fitbest* and *fitworst* are the so far best and the worst fitness of all particles; *fit(i)* represents the objective function value or the fitness of the agent *i*; and *N* is the total number of CPs. The separation distance r_{ij} between two charged particles is defined as follows:

$$\mathrm{r_{ij}} = \frac{\left\|\mathbf{X}_\mathrm{i} - \mathbf{X}_\mathrm{j}\right\|}{\left\|\left(\mathbf{X}_\mathrm{i} - \mathbf{X}_\mathrm{j}\right)/2 - \mathbf{X}_\mathrm{best}\right\| + \varepsilon} \tag{9}$$

where $\mathbf{X}_\mathrm{i}$ and $\mathbf{X}_\mathrm{j}$ are the positions of the *i*th and *j*th CPs, $\mathbf{X}_\mathrm{best}$ is the position of the best current CP, and ε is a small positive number to avoid singularities.

Step 2. CP ranking. Evaluate the values of the fitness function for the CPs, compare with each other and sort them in an increasing order.

Step 3. CM creation. Store the number of the first CPs equal to charged memory size (CMS) and their related values of the fitness functions in the charged memory (CM).

Level 2. Search

Step 1. Attracting force determination. Determine the probability of moving *i*th CP toward the *j*th CP is expressed by the following probability function:

$$p_{ij} = \begin{cases} 1 & \dfrac{\mathrm{fit(i)} - \mathrm{fitbest}}{\mathrm{fit(j)} - \mathrm{fit(i)}} > rand \ \vee fit(\mathrm{j}) > fit(\mathrm{i}) \\ 0 & \text{otherwise} \end{cases} \tag{10}$$

The value of the resultant electrical force acting on a CP is determined as:

$$\mathbf{F}_j = q_i \sum_{i,i \neq j} \left(\frac{q_i}{a^3} r_{ij} . i_1 + \frac{q_i}{r_{ij}^2} . i_2 \right) p_{ij} (\mathbf{X}_i - \mathbf{X}_j) \quad \begin{cases} j = 1, 2, \ldots., N \\ i_1 = 1, \ i_2 = 0 \Leftrightarrow r_{ij} < a \\ i_1 = 0, \ i_2 = 1 \Leftrightarrow r_{ij} \geq a \end{cases} \tag{11}$$

where q_i the volume charge density of the *j*th particle and it has a value between 0 and 1; $\boldsymbol{F}_j$ is the resultant force acting on the *j*th CP; r_{ij} is the separation distance between two charged particles which is defined as Eq. 12.

Step 2. Solution construction. Move each CP to the new position and find its velocity using the following equations:

$$\boldsymbol{X}_{j.new} = rand_{j1} . k_a . \frac{\boldsymbol{F}_j}{m_j} \Delta t^2 + rand_{j2} . k_v . \boldsymbol{V}_{j.old} \Delta t + \boldsymbol{X}_{j.old} \tag{12}$$

$$\boldsymbol{V}_{j.new} = \frac{\boldsymbol{X}_{j.new} - \boldsymbol{X}_{j.old}}{\Delta t} \tag{13}$$

where k_a is the acceleration coefficient; k_v is the velocity coefficient to control the influence of the previous velocity; and $rand_{j1}$ and $rand_{j2}$ are two random numbers uniformly distributed in the range of (0,1). Δt is the time step and set to unity. k_a and k_v are defined as:

$$k_v = 0.5(1 - iter/iter_{max}) k_a = 0.5(1 + iter/iter_{max}) \tag{14}$$

where *iter* is the actual iteration number and $iter_{max}$ is the maximum number of iterations.

Step 3. Modification of CP position. If each CP violates from its allowable boundary, its position is corrected as fallow:

$$x_{i,j} = \begin{cases} w.p.CMCR & \Rightarrow select\ a\ new\ value\ for\ a\ variable\ from\ CM, \\ & \Rightarrow w.p.(1 - PAR) do\ nothing, \\ & \Rightarrow w.p.PAR\ choose\ a\ neighboring\ value, \\ w.p.(1 - CMCR) & \Rightarrow select\ a\ new\ value\ randomly, \end{cases} \tag{15}$$

where “w.p.” is the abbreviation for “with the probability”; $x_{i,j}$ is the *i*th component of the CP *j*; The CMCR (the Charged Memory Considering Rate) varying between 0 and 1 sets the rate of choosing a value in the new vector from the historic values stored in the CM, and (1 − CMCR) sets the rate of randomly choosing one value from the possible range of values. The pitch adjusting process is performed only after a value is chosen from CM. The value (1−PAR) sets the rate of doing nothing, and PAR sets the rate of choosing a value from neighboring the best CP.

Step 4. CP ranking. Evaluate and compare the values of the fitness function for the new CPs, and sort them in an increasing order.

Step 5. CM updating. If some new CP vectors are better than the worst ones in the CM (means CPs with better merit function), include the better vectors in the CM and exclude the worst ones from the CM.

Level 3. Controlling the terminating criterion. Repeat the search level steps until a terminating criterion is satisfied. The terminating criterion is considered to be the number of iterations.

3. METHOD

In the present section the hybrid 2D-CWT and finite element model updating method is presented with the simulation of structural response data. First, the finite-element model considerations and structural response data achievement will be shown. Then, the isosurface of first displacement mode shape on (x, y) plane will be generated. Finally, the effectiveness of the proposed method for damage detection of space structures will be evaluated by applying on three types of space frames.

Step 2. Generating isosurface

First of all, the geometric pattern of space structure is modified using Formian software. the modified geometric pattern is analyzed by SAP2000 and truss element cross sections is designed according to the LRFD AISC [33]. the open-source finite-element package Opensees is used to perform an eigenvalue analysis and compute the mode shapes of the intact and damaged structures.

Secondly, the MATLAB code is written to import the displacement values of normal modes from modal analysis. The generated isosurface $f(\vec{x})$ can be directly used to indicate the location and area of the damage. In practice, this could be verified by observing that the natural frequencies and mode shapes of the structure are not drastically changed after the damage imposing event.

The 2D-CWT is implemented in MATLAB to the modified isosurface [2]. In the wavelet base damage detection methods, researchers always face with two main problems of boundary distortion and noise effects. To deal with boundary distortion, the mode shape data is extended beyond its original boundary by the cubic spline extrapolation based on points near the boundaries [15] and the noise effect of proposed wavelet analyses is treated by calculating the absolute difference values of wavelet coefficients derived from 2D-CWT analysis of intact and damaged structure as [34,35]:

$$\mathrm{D}(\vec{\mathrm{x}}) = |\mathrm{Wf_a} - \mathrm{Wf_d}| \tag{16}$$

where Wf_a and Wf_d are the 2D-CWT coefficients of intact and damaged space structure respectively. Finally by plotting the isosurface of $D(\vec{x})$ values, location and area of the damage can be defined.

Step 5. Finite element model updating

Finite element model updating technic is applied by employing the CSS algorithm to identify the damaged elements and define the severity of damage among the elements in the located region in previous step by diminishing the objective function. The objective function is formulated through the difference between the measured date of damaged structure and calculated data from the analytical model as [36]:

$$E = \sum_{i=1}^{N} \eta_i \left(\frac{\omega_i^m - \omega_i^{calc}}{\omega_i^m} \right) + \varpi \sum_{i=1}^{N} [1 - \mathrm{diag}(\mathrm{MAC}_i)] \tag{17}$$

where E is the objective function, ω_i^m and ω_i^{calc} are the natural frequencies of damaged structure and analytical model, ϖ and η_i are the weight factors of mode shape and natural frequency respectively. The subscripts *i*, denote the orders of the modes. The modal assurance criterion (MAC) is used for diagnosing global changes in vibration characteristics of a structure which can be computed as:

$$\mathrm{MAC}_i = \frac{\left| \phi_i^{m\,T} \phi_i^{calc} \right|^2}{\left(\phi_i^{m\,T} \phi_i^m \right) \left(\phi_i^{calc\,T} \phi_i^{calc} \right)} \tag{18}$$

where ϕ_i^m and ϕ_i^{calc} denote the modal vectors obtained from a damaged structure and analytical model, respectively. The subscripts *i*, denote the orders of the modes; and the superscript *T*, denotes the transpose of a vector. The damage is simulated in analytical model by diminishing the Young's modulus of elements in the damaged region located in previous step.

According to the step 4, almost 30 numbers of elements can be selected in a region with 100 centimeter radius around the local extremums in a double layer space structure. Abundance of selected elements may challenge to achieve an acceptable convergence, and it's necessary to decrease the number of elements as much as possible. In the proposed method, a loop is designed to eliminate the elements with 10% or less damage according to the results of CSS algorithm. The Flowchart of proposed method is plotted in Fig. 1.

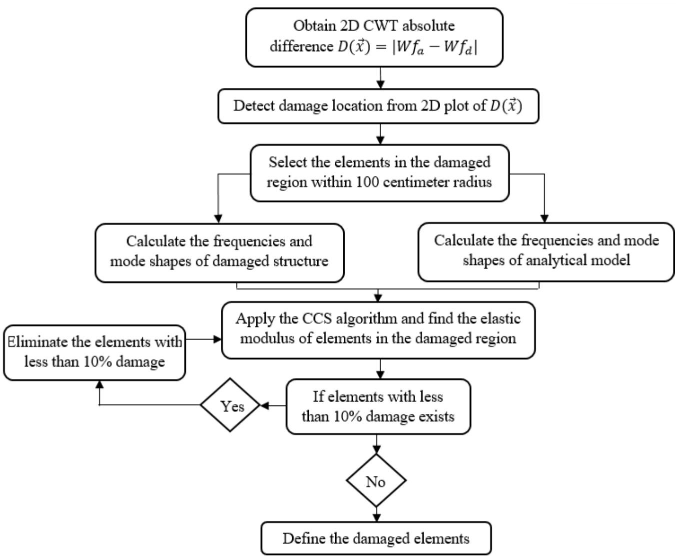

Figure 1. Flowchart of the proposed damage assessment algorithm

3. NUMERICAL EXAMPLES AND RESULTS

In order to show the capabilities of the proposed approach for identifying multiple structural damages, three illustrative type of space structures with nine different damage scenarios are considered.

Space Structure consists of steel truss elements (tubular part) and connectors (ball joint). The MERO jointing system is a multidirectional system allowing up to fourteen tubular members to be connected together at various angles. In a double-layer space structure, the ball joint system can be subjected to tension or compressive axial forces. The system consists of tubular elements that connected together by MERO jointing system. Details of connecting system and MERO ball joints are shown in Fig. 2.

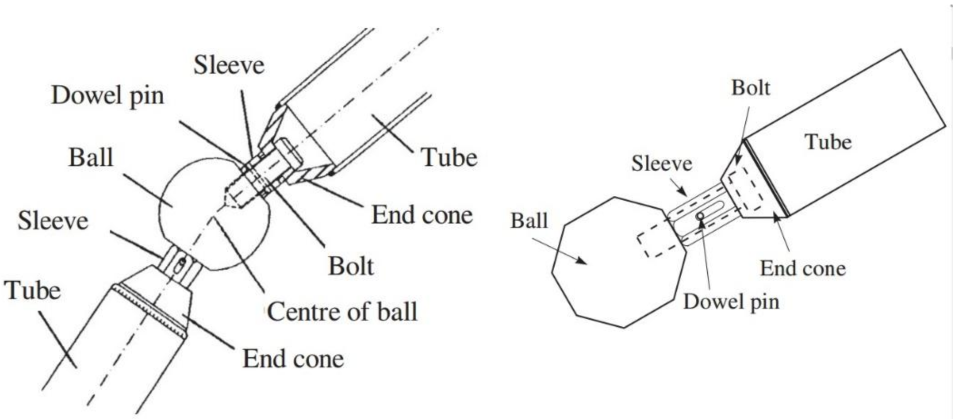

Figure 1. (a) MERO jointing system with four tubular elements; (b) member of the double layer grid; (c) details of the MERO jointing system

According to step one, a three phases design procedure is implemented to perform an eigenvalue analysis to calculate the mode shapes of space frames. The programming language Formian is utilized to create the polyhedric configuration of space frames, including node coordinates. The outcome geodesic forms of space frames are exported to SAP2000. The general views of selected space frames in SAP2000 are depicted in Fig.3.

Geometric properties of introduced double layer diamatic dome, double layer grid and double layer pyramid are illustrated in Table 1.

In the second step, the imported geometric data in SAP2000 is exploited to design structural elements. It is assumed that tubular part has uniform area and material properties along its length. This part is modeled well enough using beam element and constructed from the components which are generally utilized in practice with the modulus of elasticity $E = 200\ \mathrm{K}N/\mathrm{m}m^2$, density $\rho = 800\ kg/m^3$, yield stress $0.25\ \mathrm{K}N/\mathrm{m}m^2$ and the Poisson's ratio $\mu = 0.3$. The tubular parts are modeled by one-dimensional frame element with six degrees of freedom at each of its two nodes and designed according to the LRFD AISC [33] provision.

Table 1: The structural properties of sample systems

Frame type	Property	Value (unit)
Double layer diamatic dome	Radius of top circum sphere	50 (m)
	Radius of bottom circum sphere	48.5 (m)
	Sweep angle	40
	Frequency of top layer	16
	Number of sectors	6
Double layer grid	Length in x-direction	45 (m)
	Length in y-direction	45 (m)
	Depth of grid	1.5 (m)
	Frequency in x-direction	30
	Frequency in y-direction	30
Double layer pyramid	Length of each side of base	30 (m)
	Height of pyramid	20 (m)
	Distance between two layers	1.25 (m)
	Frequency in each side	20
	Number of sides of the base	6

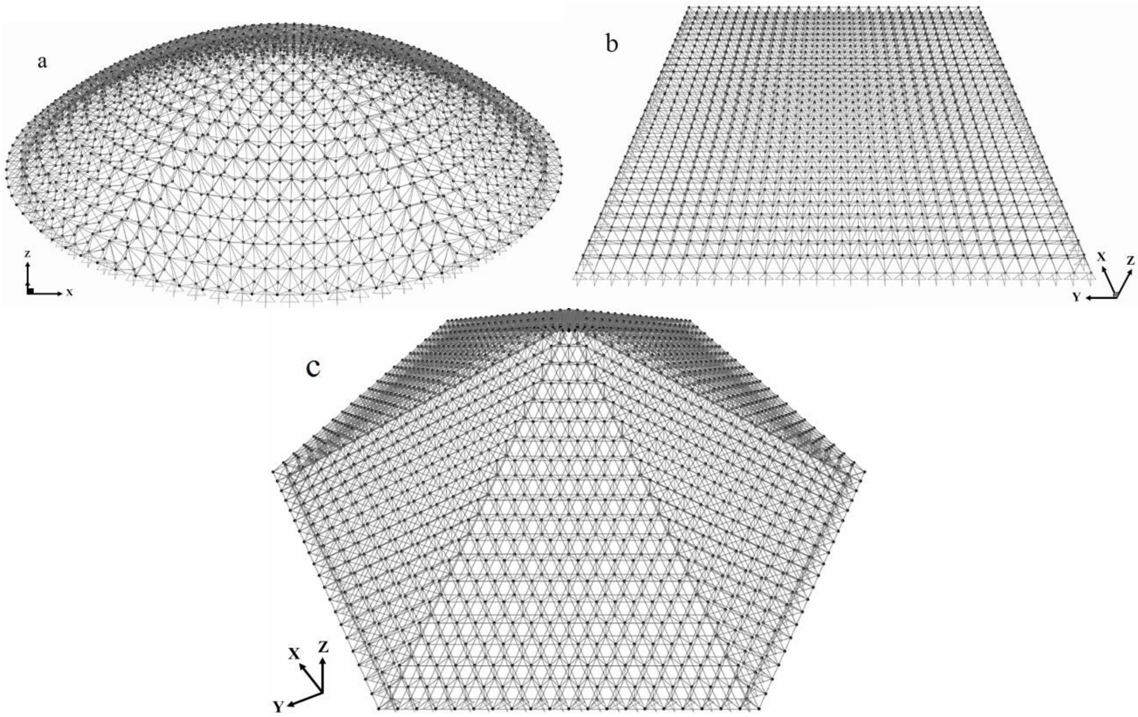

Figure 2. (a) General view of the double-layer diamatic dome for Case I; (b) general view of the double-layer grid for Case II; (c) general view of the

In the last step, the designed section properties of tubular parts and geometric properties imported from SAP2000 is used to carry out the set of modal analyses in the open-source finite-element package Opensees. The analytical Opensees model, consists of nodes coordinate, material properties and section assignments.

Opensees is used to perform an eigenvalue analysis and calculate the mode shapes of the intact and damaged space structure. Opensees software is linked to MATLAB to perform the wavelet analyses and the vertical displacement of mode shape is selected as the input data. The isosurface of first natural frequency for sample systems with equal elevation on (x, y) plane are illustrated in Fig. 4.

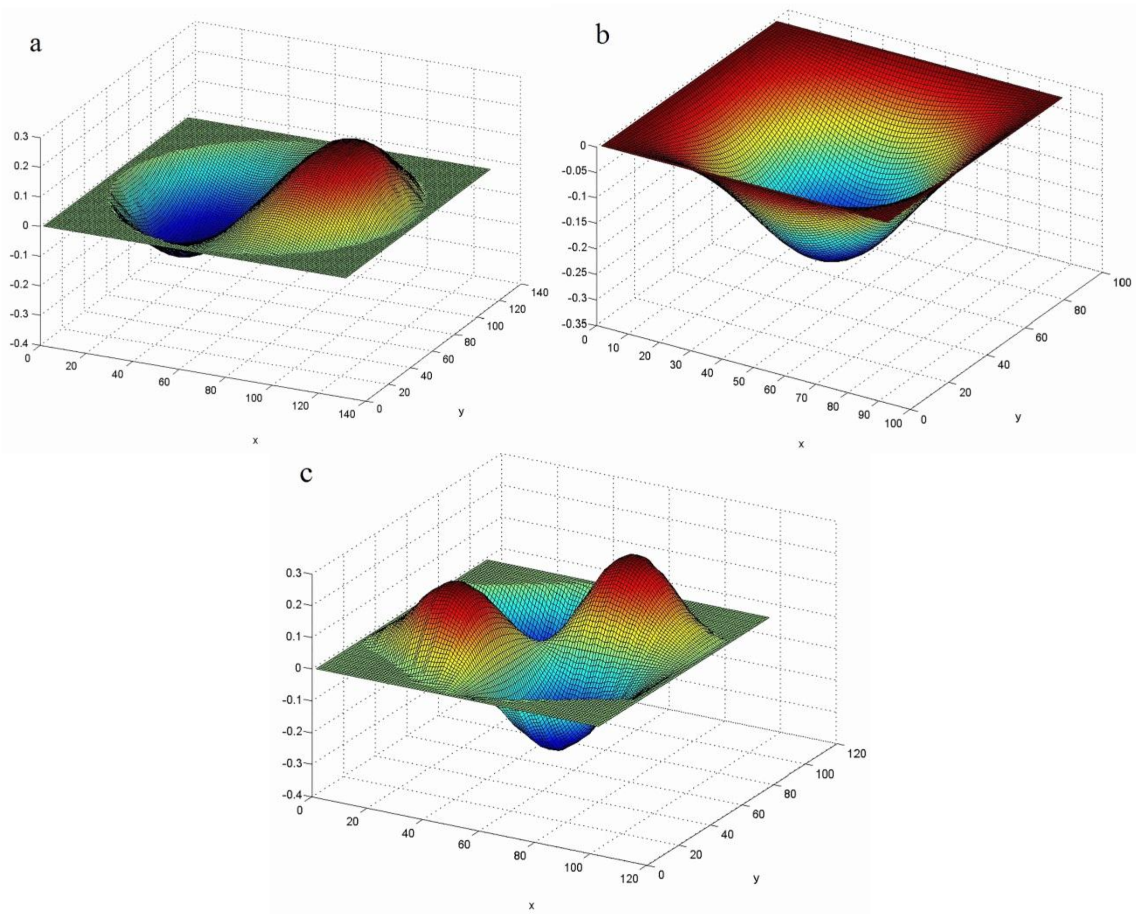

Figure 3. Isosurface of the first natural frequency for the intact model: (a) Case I; (b) Case II; (c) Case III

The 2D-CWT analysis with Mexican hat mother wavelet is applied to the isosurface generated by the fundamental mode shape. The isosurface is treated as 2D spatially distributed signals in the form of a matrix, corresponding to the vertical displacement of the joints along the x- and y-directions, respectively (table 2).

Table 2: Geometric properties of sample systems

Case No.	Matrix dimension	Number of elements	Number of joints
I	2352*2352	9216	2352
II	1861*1861	7200	1861
III	2521*2521	10980	2521

Nine damage scenarios are selected to evaluate the applicability of introduced method. Both of tubular parts and ball joints are vulnerable and could be suffered damage in a space structure. Here, damage is considered as a reduction of stiffness, which is incorporated into the equations by a reduction in the Young's modulus of damaged element. Damage can be simulated in the ball joint by a reduction in the stiffness of all its connected tubular parts. The reduction stiffness in damaged elements for all scenarios is expressed in the last column in Table 3.

Table 3: Damage scenarios of sample systems

Scenario No.	Case	Damaged elements	Damaged Joints	Coordinate on isosurface		Damage (%)
				x	y	
1	I	6391	-	52	17	50
2	I	-	1282	36	24	70
3	I	-	503	108	40	80
			1669	18	48	60
4	II	-	728	73	22	85
5	II	1121	-	28	31	90
6	II	1133		28	67	65
		1536		70	16	80
7	III	-	578	82	33	90
8	III	-	954	37	34	80
9	III	10597		58	97	100
		10599				90
		10637				80

The introduced scenarios are selected intently to investigate four main goals. Sensitivity of the proposed method to slight damage, the ability to detect damage in joints and tubular parts, multiple structural damage localization and quantification and the ability of fast damage detection for all types of space frames.

Damage index $D(x,y)$ from Eq. 19 is applied to minimize these effects. According to the denoised data modified in step 4, the final results for introduced scenarios are illustrated in Fig. 5.

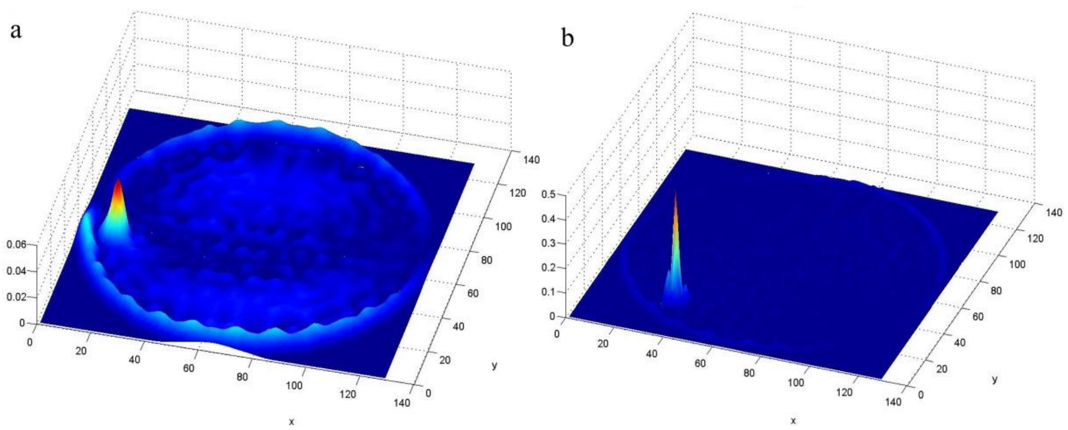

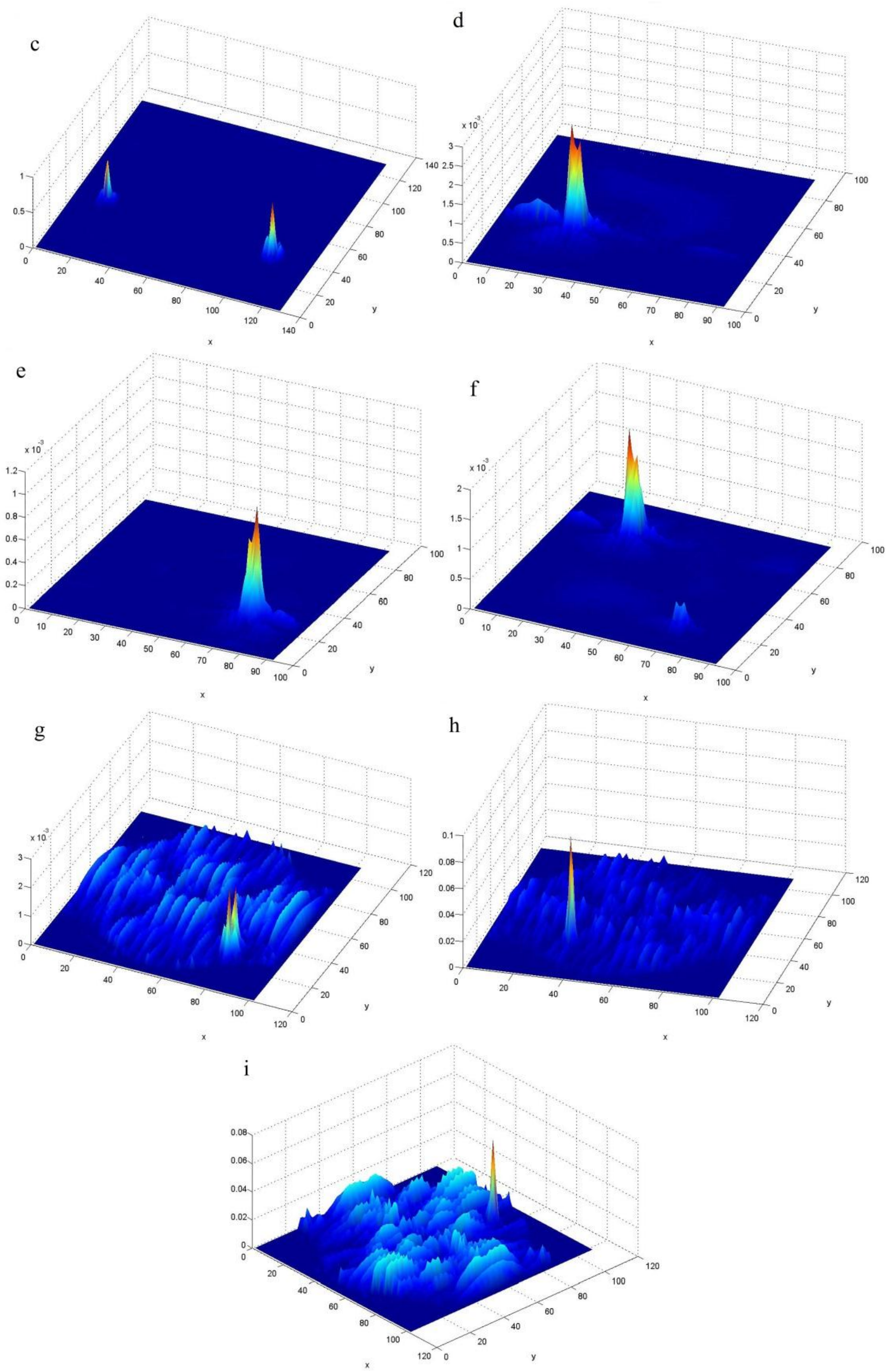

Figure 5. Damage index for the first mode shape of: (a) Scenario 1; (b) Scenario 2; (a) Scenario 3; (d) Scenario 4; (e) Scenario 5; (f) Scenario 6; (g) Scenario 7; (h) Scenario 8; (i) Scenario 9

Fig. 5 show the smoothed surface generated based on the positional damage index $D(x, y)$. The results show that, index D is a good indicator for damage detection. As the results, the noisy pattern of modified data or intensity of index D is variable and ascends according to the severity of damage imposed on the structure.

To investigating the applicability of the proposed approach on structural damage quantification, the coordinates of damages defined in the previous steps and the modal parameters (frequencies and mode shapes) of intact and damaged structure are applied as the input to the CSS algorithm. The number of modes used should be selected intently to maintain proper balance between the robustness of the algorithm, and the effort put into providing the data. While using more data helps the algorithm to converge to the right state of damage in a larger portion of runs, it generally needs considerably more effort. Here, first seven natural frequencies are considered for the assessment of damages in all Examples. The number of CPs increases the search strength of the algorithm as well as the computational cost and vice versa a small number causes a quick convergence without performing a complete search. A population of 20 CPs is used for single damage cases, and 25 CPs is used for the multiple damage cases. A maximum number of iterations of 150 are used as the termination criterion in all the examples.

Double layer diamatic dome is considered as the first numerical example. Natural frequencies for seven mode shapes of intact and damaged structures are presented in Table 3.

Table 4: Natural frequencies of the intact and damaged structures (Double layer diamatic dome-Case I)

Frequency number	Intact structure	Scenario No.		
		1	2	3
1	43.340	43.336	43.281	43.238
2	43.342	43.341	43.308	43.253
3	45.235	45.235	45.184	45.149
4	59.556	59.550	59.497	59.479
5	59.559	59.557	59.538	59.511
6	63.103	63.101	62.985	62.892
7	63.110	63.110	63.106	63.060

According to the damage coordinates, resulted from 2D-CWT analysis, 21, 21 and 40 elements is selected in scenario 1, 2 and 3, respectively to perform FEMU analysis and defining the amount of damage on elements. Variation of the objective function with the no. of iteration is shown in Fig. 6.

In the second case, Double layer grid is considered. Frequencies of the first seven mode shapes of intact and damaged structure is presented in table 5 according to the damage scenarios 4, 5 and 6.

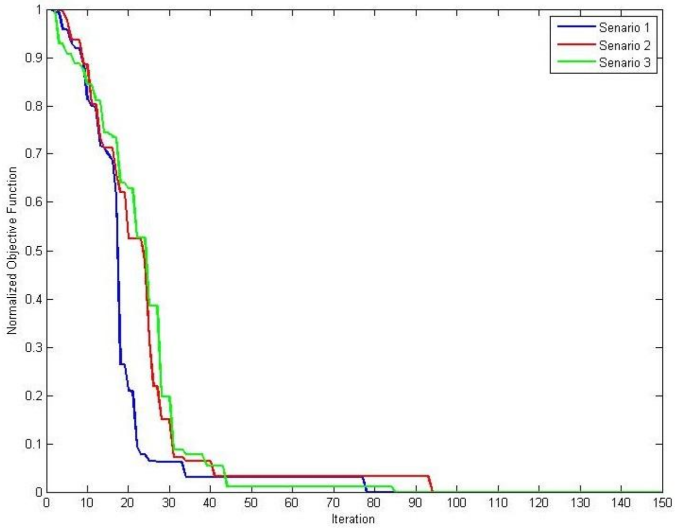

Figure 6. Variation of normalized objective function with no. of iteration for scenarios of case I

Table 2: Natural frequencies of the intact and damaged structures (Double layer grid -Case II)

Frequency number	Intact structure	Scenario No.		
		1	2	3
1	23.141	23.126	23.098	23.136
2	33.148	33.092	33.097	33.129
3	33.148	33.148	33.148	33.148
4	43.077	42.994	43.056	43.048
5	75.465	75.425	75.413	75.460
6	77.575	77.283	77.508	77.521
7	78.650	78.305	78.550	78.510

Fig. 7 shows the normalized objective function with iteration for 20, 18 and 39 selected elements in the damaged locations of scenarios 4, 5 and 6 respectively.

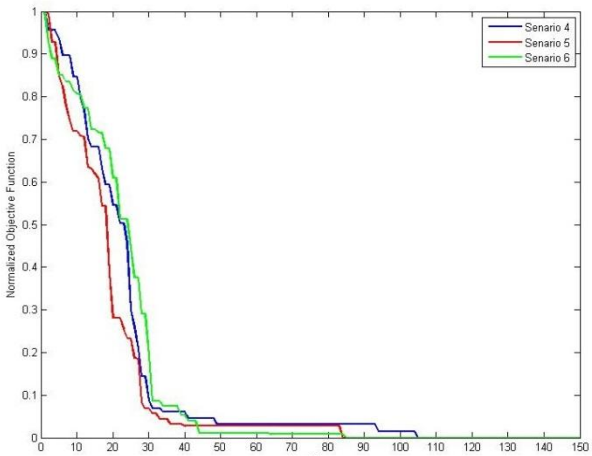

Figure 4. Variation of normalized objective function with no. of iteration for scenarios of case II

The convergence history of 24, 23 and 20 elements in the damaged locations for scenarios 7, 8 and 9 are plotted in Fig.8, respectively.

Table 3: Natural frequencies of the intact and damaged structures (Double layer pyramid - Case III)

Frequency number	Intact structure	Scenario No.		
		1	2	3
1	58.928	58.853	58.844	58.907
2	58.928	58.918	58.922	58.928
3	66.444	66.360	66.344	66.408
4	66.445	66.406	66.397	66.445
5	74.373	74.300	74.291	74.353
6	84.616	84.549	84.597	84.614
7	94.102	93.977	93.958	94.034

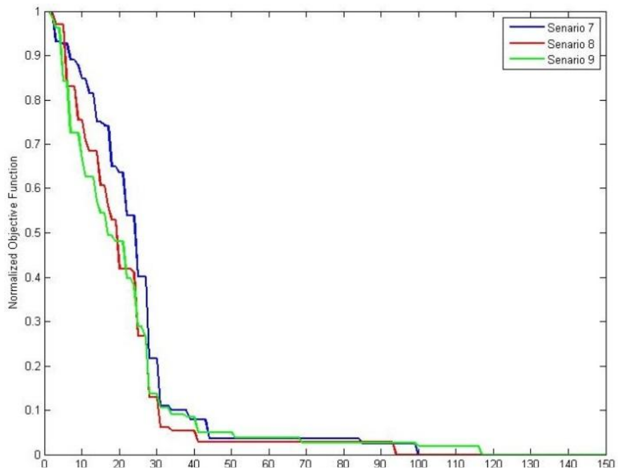

Figure 5. Variation of normalized objective function with no. of iteration for scenarios of case III

According to the results of FEMU, error from the exact damage for each element in the damaged region defined by 2D-CWT is illustrated in Fig. 9 for scenario 1. It is worth to remind here that the more distant from zero these plots are, the worse the performance of a given algorithm is.

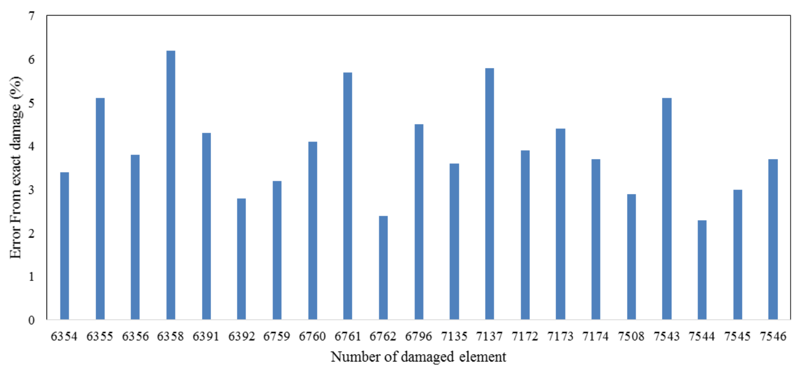

Figure 6. Errors from the exact damage of elements in scenario 1

The mean error from exact damage for all damage scenarios are plotted in Fig. 10.

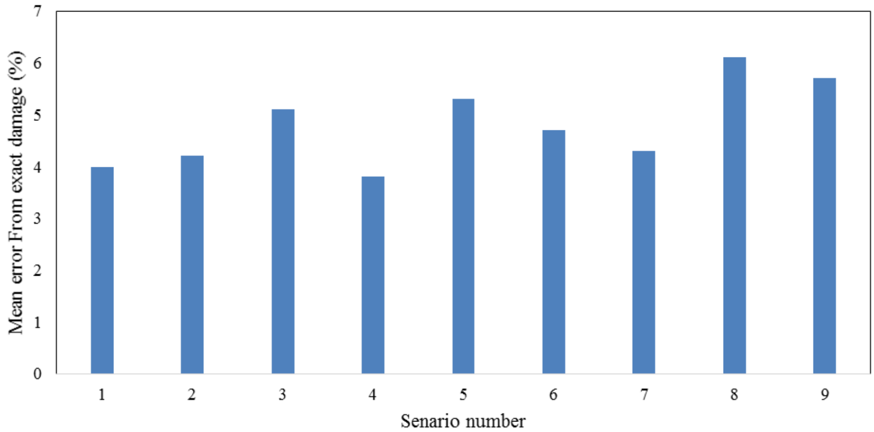

Figure 7. The mean error from exact damage for all damage scenarios

The results reveal that the applied optimization algorithm and proposed FEMU method is completely capable of multiple damage localization in different types of space structures.

4. CONCLUSIONS

The main objective of this heuristic study is to evaluate the performance of an evolutionary strategy in the finite element model updating approaches for damage assessment in space structures. Based on the continuous wavelet transform, the location of damaged joints or tubular parts are defined according to mode shapes of damaged and intact structure to increase the calculation costs of damage assessment. The finite element model updating method has been implemented as an inverse optimization problem by applying the charged system search algorithm to assess the severity of damage in each element sited in the damage region.

Nine different numerical examples on three different shape of space structure were studied in order to show the advantages of proposed method. Referring to the results of these examples, the usefulness, Simplicity and flexibility of the proposed method in defining the amount of elements damage is demonstrated.

The numerical results demonstrate that the combination of the 2D-CWT algorithm together with finite element model updating concepts can provide an efficient tool for properly identifying the multiple damages in all types of space structures without any limitation on size and shape of structure.

REFERENCES

1. Kaveh A, Zolghadr A: An improved CSS for damage detection of truss structures using changes in natural frequencies and mode shapes, *Adv Eng Softw* 2015; **80**: 93-100.
2. Gholizad A, Safari H: Two-dimensional continuous wavelet transform method for

multidamage detection of space structures, *J Perform Construct Facili* 2016, **13**(3) DOI: 10.1061/(ASCE)CF.1943-5509.0000924.
3. Roveri N, Carcaterra A. Damage detection in structures under traveling loads by Hilbert–Huang transform, *Mech Syst Signal Process* 2012, **28**: 128-44.
4. Quek ST, Tua PS, Wang Q: Detecting anomalies in beams and plate based on the Hilbert–Huang transform of real signals, *Smart Mater Struct* 2003, **12**: 447.
5. Xu W, Radzieński M, Ostachowicz W, Cao M. Damage detection in plates using two - dimensional directional Gaussian wavelets and laser scanned operating deflection shapes, *Structural Health Monitor* 2013; **12**(5-6) 457-68.
6. Yun GJ, Lee SG, Carletta J, Nagayama T. Decentralized damage identification using wavelet signal analysis embedded on wireless smart sensors, *Eng Struct* 2011, **33**: 2162-72.
7. Bharathi Priya C, Likhith Reddy A. Low frequency and boundary condition effects on impedance based damage identification, *Case Studies Nondestructive Test Evaluat* 2014; **2**: 9-13.
8. Hamzeloo SR, Shamshirsaz M, Rezaei SM. Damage detection on hollow cylinders by electro-mechanical impedance method: experiments and finite element modeling, *Comptes Rendus Mécanique* 2012; **340**: 668-77.
9. Strang G, Nguyen T. *Wavelets and Filter Banks*, SIAM, 1996.
10. Haar A. Zur Theorie der orthogonalen Funktionensysteme, *Mathemat Annalen* 1910, **69**: 331-71.
11. Surace C, Ruotolo R. Crack detection of a beam using the wavelet transform. In *The International Society for Optical Engineering, Poit International Society for Optical* 1994: 1141-47.
12. Zhong S, Oyadiji SO: Detection of cracks in simply-supported beams by continuous wavelet transform of reconstructed modal data, *Comput Struct* 2011, **89**: 127-48.
13. Song YZ, Bowen CR, Kim HA, Nassehi A, Padget J, Gathercole N, Dent A: Non-invasive damage detection in beams using marker extraction and wavelets, *Mech Systems Signal Process* 2014; **49**: 13-23.
14. Xiang J, Liang M: Wavelet-based detection of beam cracks using modal shape and frequency measurements, *Comput-Aided Civil Infrastruct Eng* 2012; **27**: 439-54.
15. Fan W, Qiao P. A 2-D continuous wavelet transform of mode shape data for damage detection of plate structures, *Int J Solids Struct* 2009; **46**: 4379-95.
16. Katunin A. Damage identification in composite plates using two-dimensional B-spline wavelets, *Mech Syst Signal Process* 2011, **25**: 3153-67.
17. Xu W, Cao M, Ostachowicz W, Radzieński M, Xia N: Two-dimensional curvature mode shape method based on wavelets and Teager energy for damage detection in plates, *J Sound Vib* 2015, **347**: 266-78.
18. Xiang J, Matsumoto T, Wang Y, Jiang Z: Detect damages in conical shells using curvature mode shape and wavelet finite element method, *Int J Mech Sci* 2013, **66**: 83-93.
19. Baneen U, Kinkaid NM, Guivant JE, Herszberg I: Vibration based damage detection of a beam-type structure using noise suppression method, *J Sound Vib* 2012, **331**: 1777-88.
20. Makki Alamdari M, Li J, Samali B: FRF-based damage localization method with noise suppression approach, *J Sound Vib* 2014, **333**: 3305-20.
21. Avci O, Abdeljaber O. Self-organizing maps for structural damage detection: a novel

unsupervised vibration-based algorithm, *J Perform Construct Facilit* 2015, 0:04015043.
22. Doebling SW, Farrar CR, Prime MB, Shevitz DW. Damage identification and health monitoring of structural and mechanical systems from changes in their vibration characteristics: A literature review, In *Other Information: PBD: May 1996*, Edited by; 1996: Medium: ED; Size: 132 p.
23. Majumdar A, Maiti DK, Maity D: Damage assessment of truss structures from changes in natural frequencies using ant colony optimization, *Appl Math Comput* 2012, **218**: 9759-72.
24. Ding ZH, Huang M, Lu ZR: Structural damage detection using artificial bee colony algorithm with hybrid search strategy, *Swarm Evolutionary Comput* 2016, 28:1-13.
25. Seyedpoor SM. A two stage method for structural damage detection using a modal strain energy based index and particle swarm optimization, *Int J Non-Linear Mech* 2012, **47**: 1-8.
26. Shayanfar MA, Kaveh A, Eghlidos O, Mirzaei B: Damage detection of bridge structures in time domain via enhanced colliding bodies optimization, *Int J Optim Civil Eng* 2016, **6**: 211-26.
27. Shiradhonkar SR, Shrikhande M: Seismic damage detection in a building frame via finite element model updating, *Comput Struct* 2011; **89**: 2425-38.
28. Fu YZ, Lu ZR, Liu JK: Damage identification in plates using finite element model updating in time domain, *J Sound Vib* 2013, **332**: 7018-32.
29. Nhamage IA, Lopez RH, Miguel LFF: An improved hybrid optimization algorithm for vibration based-damage detection, *Adv Eng Softw* 2016, **93**: 47-64.
30. Kaveh A, Talatahari S: A novel heuristic optimization method: charged system search, *Acta Mech* 2010; **213**: 267-89.
31. Rucka M, Wilde K: Application of continuous wavelet transform in vibration based damage detection method for beams and plates, *J Sound Vib* 2006, **297**: 536-50.
32. Hildreth EC. Computations underlying the measurement of visual motion, *Artificial Intell* 1984, **23**: 309-354.
33. AISC: Resistance factor design specification for structural steel buildings, Edited by Chicago: American Institute of Steel Construction, 1999.
34. Gallego A, Moreno-García P, Casanova CF: Modal analysis of delaminated composite plates using the finite element method and damage detection via combined Ritz/2D-wavelet analysis, *J Sound Vib* 2013, 332:2971-2983.
35. Castro E, García-Hernandez MT, Gallego A. Damage detection in rods by means of the wavelet analysis of vibrations: Influence of the mode order, *J Sound Vib* 2006, **296**: 1028-38.
36. Marwala T. *Finite Element Model Updating Using Computational Intelligence Techniques: Applications to Structural Dynamics*, Springer Science & Business Media, 2010.